APS physics

CHORUS

This is the accepted manuscript made available via CHORUS. The article has been published as:

Encoding the structure of many-body localization with matrix product operators

David Pekker and Bryan K. Clark

Phys. Rev. B **95**, 035116 — Published 10 January 2017

DOI: 10.1103/PhysRevB.95.035116

Encoding the structure of many-body localization with matrix product operators

David Pekker[1] and Bryan K. Clark[2]
[1]*Department of Physics and Astronomy, University of Pittsburgh*
[2]*Department of Physics, University of Illinois at Urbana Champaign*

Anderson insulators are non-interacting disordered systems which have localized single particle eigenstates. The interacting analogue of Anderson insulators are the Many-Body Localized (MBL) phases. The spectrum of the many-body eigenstates of an Anderson insulator is efficiently represented as a set of product states over the single-particle modes. We show that product states over Matrix Product Operators of small bond dimension is the corresponding efficient description of the spectrum of an MBL insulator. In this language all of the many-body eigenstates are encode by Matrix Product States (i.e. DMRG wave function) consisting of only two sets of low bond-dimension matrices per site: the G_i matrices corresponding to the local ground state on site i and the E_i matrices corresponding to the local excited state. All 2^n eigenstates can be generated from all possible combinations of these sets of matrices.

The interacting analogue of the Anderson insulator[1,2] is many-body localization as first suggested by a diagrammatic calculation[3,4]. Significant recent interest has gone to understanding whether many-body localized (MBL) phases exist as well as determining their properties[5–18]. Many-body localized phases are believed to have a number of unusual properties including: (a) perfect zero conductivity at finite temperature, (b) failure to thermalize, and (c) a large number of local constants of motion and corresponding conserved quantities. For MBL systems with a thermally-driven (or more precisely energy-density-driven) transitions these features persist all the way to the critical energy density.

The MBL phase transition is unique in that the phase transition is dynamical and, therefore, not simply a feature of the ground state wave-function or finite temperature density matrix. Instead, the MBL phase transition is believed to be caused by a qualitative change in the finite energy density eigenstates of the Hamiltonian. In fact, there have been significant previous work showing that eigenstates of MBL phases are special. These eigenstates have poisson statistics[12] and individual eigenstates obey area laws ([13,19–21]. As a corollary they can be represented by matrix product states[6,22]; by finite dimensional MPO applied to a product state in the physical basis; by a finite depth quantum circuits[13]; or by an RG procedure which truncates at finite flow time[20,21,23].

Like MBL eigenstates, the many-body eigenstates in an Anderson insulator have atypical properties. In addition, though, they have a very simple form: a product state over localized single-particle eigenstates. Importantly, this means that for an L-site lattice, L single particle localized orbitals is sufficient knowledge to generate every many-body eigenstate. From this simple form, many of the properties of Anderson insulators can be understood. This leads us to a simple question: Do the many-body eigenstates of a MBL phase also share a simple and concise form?

The primary result of this letter is to show that the matrix product states which represent MBL eigenstates have a simple uniform structure over the whole spectrum. To manifest this structure, we describe Anderson insulators and then show a natural generalization of the Anderson insulator case for the MBL case. Consider the specific example of one dimensional disordered spin-1/2 chains. In the non-interacting case, we can work in the basis of single particle eigenfunctions. Moreover, since all eigenfunctions are localized we can assign each eigenfunction to a lattice site i. Hence, each state of the many-body spectrum corresponds to a product state in which we assign each site of the lattice either $\{\psi_i = 0, \phi_i = 1\}$ if the corresponding single particle state is empty or $\{\psi_i = 1, \phi_i = 0\}$ if it is occupied

$$\Psi_{\text{Anderson}} = \prod_i (\psi_i |e_i\rangle + \phi_i |g_i\rangle). \tag{1}$$

A natural extension of these product states to the interacting but localized regime is obtained by replacing the the localized single particle orbitals e_i and g_i by tensors of finite bond dimension $E^{\sigma_i}_{i,jk}$ and $G^{\sigma_i}_{i,jk}$, where the indices j and k are dummy indices that are summed over when contracting the tensors. The index σ_i corresponds to the local spin state on site i, which we will choose to be defined in the original Fock basis. While these tensor states can encode some short distance entanglement, just like product states, they cannot encode long distance entanglement. We give evidence that in the MBL phase all eigenstates can be compactly represented in the from

$$\Psi_{\text{MBL}} = \prod_i (\psi_i E^{\sigma_i}_i + \phi_i G^{\sigma_i}_i)|\sigma_i\rangle. \tag{2}$$

Hence, the MBL ground state corresponds to the Matrix Product State (i.e. DMRG wave function)

$$\Psi_{\text{MBL},000\ldots} = \sum_{jkl\ldots} G^{\sigma_1}_{1,j} G^{\sigma_2}_{2,jk} G^{\sigma_1}_{3,kl} \ldots |\sigma_1\sigma_2\sigma_3\ldots\rangle. \tag{3}$$

Swapping $G^{\sigma_i}_{i,jk}$ for $E^{\sigma_i}_{i,jk}$ creates a local excitation of the system.

$$\Psi_{\text{MBL},010\ldots} = \sum_{jkl\ldots} G^{\sigma_1}_{1,j} E^{\sigma_2}_{2,jk} G^{\sigma_1}_{3,kl} \ldots |\sigma_1\sigma_2\sigma_3\ldots\rangle. \tag{4}$$

The full many-body spectrum can be obtained by composing all combinations of $G^{\sigma_i}_{i,jk}$'s and $E^{\sigma_i}_{i,jk}$'s on all sites, thus mapping product states onto matrix product states. We show that these matrices can be directly identified from the Matrix Product Operator (MPO) derived from the unitary transformation that diagonalizes the Hamiltonian of our MBL system. Remarkably, we find strong numerical evidence that inside the

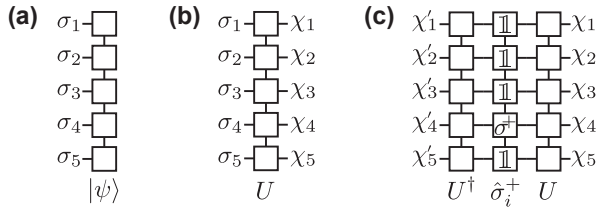

FIG. 1. Diagram of (a) a matrix product state $|\psi\rangle$, (b) a matrix product operator U, and (c) the operator product $U^\dagger\hat{\sigma}_i^+U$. The boxes correspond to tensors and lines to tensor indices. Lines connecting two boxes are indices to be contracted while dangling lines are external indices. The matrix product state $|\psi\rangle$ "eats" the external indices $|\sigma_1\sigma_2\sigma_3\ldots\rangle$ (these are the configurations of our spin-1/2 chain) and "spits" out a complex number – the amplitude of that configuration. Similarly, the matrix product operator "eats" two sets of external indices – the "ket" set & the "bra" set – and "spits" out the value of the corresponding matrix element.

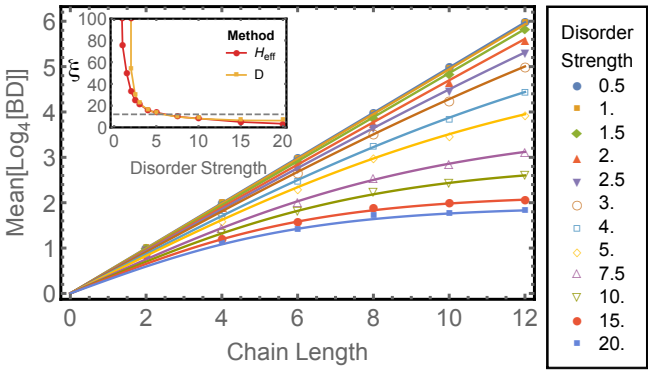

FIG. 2. Saturation of the Bond Dimension D of the Matrix Product Operator representing the unitary that diagonalizes the Hamiltonian as a function of the Chain Length for a number of values of disorder strength. D was measured on the middle bond. Points represent numerical data (from 200 disorder realizations) and the solid lines are fits (see text). The change of regime – saturating D vs. growing D – corresponds to the transition from the localized to the delocalized phase. Inset: Length ξ as a function of disorder strength, computed using (1) the decay of couplings in the effective Hamiltonian H_{eff} and (2) the saturation of D [to match (1) and (2) we scaled $\xi_{H_{\text{eff}}} \to 8.7 * \xi_{H_{\text{eff}}}$]. Dashed line indicates maximum chain length ($L = 12$).

MBL phases this MPO is efficiently representable: the typical bond dimension of the tensors $G^{\sigma_i}_{i,jk}$ and $E^{\sigma_i}_{i,jk}$ saturates at a finite value even as the system size increases.

An introduction to Matrix Product States and Operators – Here we review the essential aspects of MPS/MPO (for a more in-depth review see, e.g., Ref. 24). A convenient way to depict matrix product states and operators is shown in Fig. 1. For the case of spin-1/2 chains, the external indices can take on two values $\sigma_i, \chi_i \in \{|\uparrow\rangle_i, |\downarrow\rangle_i\}$. On the other hand the internal indices can span the range $\{1,\ldots,D_i\}$, where D_i is the "bond dimension" for the bond between site i and $i+1$. The value of D_i is a tuning parameter that controls how much entanglement can be carried by the internal index linking neighboring sites. To describe eigenstates of strongly disordered systems we allow each internal bond to have a different bond dimension as dictated by the disorder realization.

To summarize, an MPS for an L-site chain is parametrized by $2L$ matrices – two matrices per site $M^{\uparrow}_{i,k_ik_{i+1}}$ and $M^{\downarrow}_{i,k_ik_{i+1}}$. Analogously, an MPO contains four matrices for each site i: $O^{\uparrow\uparrow}_{i,k_ik_{i+1}}$, $O^{\uparrow\downarrow}_{i,k_ik_{i+1}}$, $O^{\downarrow\uparrow}_{i,k_ik_{i+1}}$, and $O^{\downarrow\downarrow}_{i,k_ik_{i+1}}$.

A unitary operator U, which diagonalizes a Hamiltonian, maps the eigenstates of the Hamiltonian to the product states (i.e. bit strings of length L). Consider the action of the MPO representing U on the MPS representing the product state $|p\rangle$. The MPS has $D = 1$, thus the resulting MPS, $U|p\rangle$, simply selects two of the four MPO matrices per site. Hence, all the eigenstates of the Hamiltonian are encoded by matrix product states generated from all combinations of the matrices $O^{\downarrow\sigma_i}_i$ and $O^{\uparrow\sigma_i}_i$. We then choose G_i and E_i to be $O^{\downarrow\sigma_i}_i$ or $O^{\uparrow\sigma_i}_i$ depending on whether the product state which maps to the ground state has $\downarrow$ or $\uparrow$ on site i. Notice that all eigenstates of the system are represented by $4L$ matrices (those that make up the MPO). The key question that we address is whether the MPO which represents the unitary operator can be represented by matrices with a fixed bond dimension that is independent of the system length L.

Small bond dimension MPO – The strategy that we employ for testing whether MPOs can efficiently describe the unitary transformation that takes product states to eigenstates consists of three steps: (1) we construct the exact unitary transformation using exact diagonalization, (2) we identify a correspondence between the exact eigenstates and product states which maximally preserves locality, and (3) we compress the transformation into a matrix product operator. We test this approach on a spin 1/2 chain with the Hamiltonian

$$H = \sum_{\langle i,j\rangle} S_i \cdot S_j + \sum_i h_i S^z_i \tag{5}$$

where h_i is a random field chosen from a distribution $h_i \in [-\Delta, \Delta]$. The location of the MBL transition in H, as a function of Δ, is still not fully established[12,25]. The current best lower bound is at $\Delta \gtrsim 4$[25]. In our strategy, there is a clear notion of optimality: the procedure that produces an MPO with the smallest bond dimension. This hinges on correctly identifying the spatial position of the excitations in each exact eigenstate and matching these locations to the corresponding product state. Finding the optimal matching is a numerically challenging task and hence we use a heuristic procedure. The bond dimensions we obtain are therefore an upper bound to the best MPO bond dimensions.

To find the matching between the list of eigenvectors $|e\rangle$ and product states $|p\rangle$ we use the intuition that each eigenstates of the strongly localized interacting system should have a considerable overlap with its parent state – an eigenstate of the non-interacting system[3]. In our case, the non-interacting system corresponds to Hamiltonian (5) without the Heisenberg coupling, hence the parent states are the product states. For the case of weak interactions (large Δ) this heuristic gives a one-to-one and onto mapping $f(|e\rangle) = |p\rangle$ between eigenstates and product states. However, generically, the heuristic can map multiple eigenstates to the same product state – a sit-

uation that requires further resolution.

For the generic case we construct the table $M(|e\rangle, |p\rangle) = |\langle e|p\rangle|^2$ of overlaps between eigenstates and product states. A one-to-one and onto mapping $f(|e\rangle) = |p\rangle$ is defined by selecting one entry from each row of $M(|e\rangle, |p\rangle)$ with the constraint that each column also has only one selection. To get the best total overlap between eigenstates and product states our goal becomes to maximize the sum of the selected entries $\sum_e M(|e\rangle, f(|e\rangle))$. This maximization can be re-written as a graph problem where product states and excited states represent nodes on two halves of a bipartite graph and their overlap is a weighted edge between them. Our objective function then reduces to finding the maximum weighted bipartite matching in this graph. This problem is solved in $O(n^3)$ by the the Hungarian algorithm[26].

Having performed the bipartite matching, we re-order the columns of U so that the eigenstates appear in the same order as the product states (which are represented by the rows of U). Next, we perform a gauge fixing step – the eigenvectors that we found have a random sign that we correct by flipping the sign of each eigenvector such that all of the diagonal elements of U are positive. Having encoded 'locality' into U, we compress it into an MPO following the standard prescription[24].

The accuracy of our MPO is controlled by smallest singular values kept during the compression. In the MBL phase, we find only few singular values above the cut-off and hence the resulting MPO has a small bond dimension; while in the ergodic, there are many more singular values above the cut-off and hence the bond dimension of the resulting MPO is large.

Numerical Results – The main result of our manuscript is depicted in Fig. 2. In this figure, we plot the bond dimension D of the MPO representing the unitary that diagonalizes the Hamiltonian (5) as a function of system size L for various disorder strengths Δ[27]. We have averaged the $\log_4[D]$ over 200 disorder realizations. As we are averaging the logarithm of the bond dimension, rare regions do not have a disproportionate affect on the average. From the figure, we observe that for systems with weak disorder ($\Delta \lesssim 3$) the logarithm of the bond dimension grows linearly with system size, while for those with strong disorder ($\Delta \gtrsim 7.5$) the bond dimension has saturated by the time the chain length has reached $L = 12$. For disorder strengths $3 \lesssim \Delta \lesssim 7.5$ we do not have access to long enough chains to make a qualitative statement.

We can, however, quantify the saturation effect by fitting the D vs. L curves with a generic saturation function: $\log_4[D(L)] = a \tanh(L/\xi)$ where a and ξ are the fitting parameters. In the inset of Fig. 2 we plot the saturation length scale ξ as a function of the bond dimension. We observe that for systems with $\Delta \gtrsim 5$ the saturation length-scale is indeed shorter than the system size. As the disorder becomes weaker, ξ quickly surpasses the system size (at which point we can no longer accurately measure it), indicating the end of the MBL phase. It is important to note that the supremum over the bond dimensions of all eigenstates is a lower bound on the bond dimension of U. Therefore it is not surprising that the lengths scales and bond dimensions we find are longer than those obtained for typical eigenstates[13].

An alternative way to compute ξ is using the effective Hamiltonian of reference[10]. In the product basis, the Hamiltonian (5) acquires the form

$$H_{\text{eff}} = \sum_i J_i \sigma_i^z + \sum_{i,j} J_{i,j} \sigma_i^z \sigma_j^z + \sum_{i,j,k} J_{i,j,k} \sigma_i^z \sigma_j^z \sigma_k^z + \dots . \quad (6)$$

We generate H_{eff} by solving $Ax = b$ for x where $x = \{1, h_1, h_2, ..., J_{12}, J_{13}, ...\}$ and A is the matrix that relates this set of couplings to the exact eigenvalues via the l-bit configurations. In the MBL phase all couplings $J_{i,j}$, $J_{i,j,k}$, ... must decay as a function of the separation $|i - j|$. We use this fact to our advantage to extract ξ from the decay of $J_{i,j}$. We find that, up to a fixed rescaling by the factor 8.7, the two definitions of ξ seem to match [see Inset Fig 2].

To summarize, our main result is that for systems in the MBL phase the full spectrum of eigenvectors can be described using an MPO of low bond dimensions. This observation dictates the structure of the many-body eigenstates. The MPO representation quantifies the notion of localized excitations and therefore dictates such properties as lack of thermalization, entanglement, emergent integrability, etc.

To understand the nature of the break down of the MPO representation, we look at the distribution of bond dimensions at fixed disorder strength Fig. 3(a). In the strongly localized matter, we find that the distribution of bond dimensions tends to be strongly peaked around $D = 1$ (the minimum possible value for D). As the disorder strength decreases, we observe that (1) the peak in the distributions is starting to shift to small but finite values of D associated with a growing localization length, and (2) the emergence of a power law tail in the distributions [see Fig. 3(b)]. This power law tail signifies the onset of Griffiths physics: the system contains exponentially rare regions of the delocalized phase that give an exponentially strong contribution to the bond dimension. Griffiths physics have been seen in similar quantities such as the entanglement of individual eigenstates by ref.[11,13,15]. As the disorder strength decreases the Griffith regions become less rare. At the transition point we see a drastic change in the distribution of D as it becomes extremely broad. Similar broadening has been observed in entanglement entropies of single eigenstates[15]. On the delocalized side of the transition the distribution again becomes sharply peaked, but this time around a system size dependent value. The broadening of the distribution at the transition point indicates that the mechanism that drives the delocalization transition is the formation of resonances between the rare regions.

Discussion – The fact that the unitary that diagonalizes the Hamiltonian can be compressed into an MPO of small bond dimension has direct consequences for the properties of the MBL phase. We begin by noting that the typical entanglement entropy of any of the eigenstates is finite as it is limited by $\log[D]$ which contradicts ETH. Within our framework we can rule out thermalization without appealing to ETH. Consider a local operator such as $U\sigma_i^+ U^\dagger$. Note this is the l-bit raising operator[10] in the MPO language. The application of the MPO composed from $UU^\dagger$ and the MPO composed from $U\sigma_i^+ U^\dagger$ differ only on a single site [see Fig. 1(c)]. As the matrix on this site has a bond dimension which doesn't grow with sys-

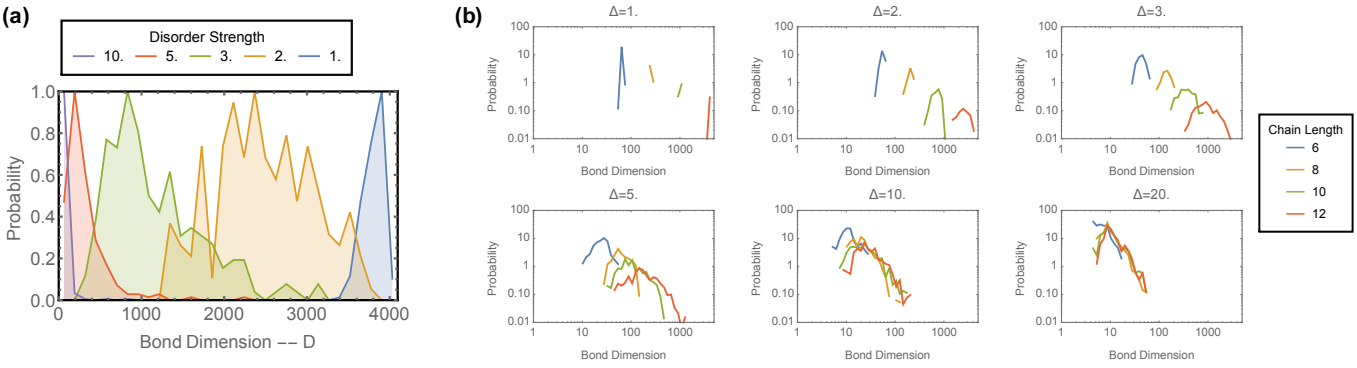

FIG. 3. The Probability Distribution Function (PDF) of the bond dimension across the center bond of the spin chain. (a) PDF for 12-site chains at various disorder strengths. For weak disorder, $\Delta = 1$, the PDF is clustered around the maximal allowed value $D = 4^6 = 4096$. Near the many-body localization-delocalization transition, $\Delta = 3$, the PDF becomes spread over a wide range of bond dimensions. In the localized phase, the PDF becomes clustered around the $D = 4^\xi$ with a power law tail extending to larger bond dimensions. (b) PDF for chains of various length and disorder strengths, power laws can be observed for $\Delta \gtrsim 3$.

tem size, it will connect single eigenstates to a sub-extensive number of eigenstates all of which must have similar matrices far from the operator application (similar arguments that utilize the locality of the unitary as opposed to the G/E structure of the eigenstates have been presented in Refs. 10 and 13). This fact tells us that (1) there is no thermalization as a local kick to the system remains local; (2) there is no electrical conductivity as an excitation injected into the system at site i remains put for very long times; and (3) there is no level repulsion as excitations from spatially distant operators σ_i^+ and σ_j^+ have no overlap.

The MPO language lets us explicitly write the emergent local constants of motion. A constant of motion is a hermitian operator which commutes with the Hamiltonian. Consider operators of the form

$$\rho_{\text{product}} = I_1 \otimes \ldots I_{k-1} \otimes \sigma_k^z \otimes I_{k+1} \ldots I_n = \sum_p \alpha_p |p\rangle\langle p| \quad (7)$$

where $|p\rangle$ is a product state over all the sites. Applying the MPO U to this operator gives us $U\rho_{\text{product}}U^\dagger = \sum_i \alpha_i |e_i\rangle\langle e_i|$ where $|e_i\rangle$ are eigenstates of the many-body system. Operators of this form commute with the Hamiltonian and consequently are constants of motion. Mirroring our previous argument, as $U\rho_{\text{product}}U^\dagger$ differ from $UU^\dagger$ by a single matrix they have an exponential weak effect on distant parts of the system and hence the constants of motion we've written down are local.

Finally we remark that the application of MPOs as a variational basis for diagonalizing many-body localized Hamiltonians has not escaped our notice. There has been considerable work on using MPS as a variational basis for individual eigenstates[28–32] and the extension to MPOs is natural. Indeed, our numerics indicates that in the localized phase we can represent the entire spectrum of eigenstates of the Hamiltonian in a compact form using an MPO of low bond dimension. Due to the compact nature of the MPO representation it should be possible to diagonalize the Hamiltonian of rather large systems, significantly beyond the limits of exact diagonalization. The Griffiths effects will control the success of this endeavor. Specifically, each disorder realization will have rare regions of lower than typical disorder that will require an exponentially large bond dimension. The probability to find a rare region of length l in a chain of length L scales as $L\exp(-l/\xi)$. Therefore, with probability 1 a chain will contain a rare region that requires $D \propto L^\xi$, which is a much softer constraint than the typical exponential scaling for exact diagonalization. We point out that having the complete spectrum will allow for efficient evaluation of finite energy density and dynamical properties of these systems. In fact, during the refereeing process of this paper two groups have made progress on the this program of variationally optimizing MPOs[33,34].

In this work, we have focused on elucidating a structure for the entire spectrum of eigenstates that is analogous to the structure that is seen in Anderson localization. We have additionally seen that the structure of these eigenstate gives us a way to understand the properties of the MBL phase. Although we have focused here primarily on one-dimensional system, there is every reason to believe that the natural generalization where PEPS replace MPS will hold for higher dimensions.

We thank Vadim Oganesyan, David Huse, Bela Bauer, and Chetan Nayak for useful discussions. We thank Vedika Khemani for pointing out a discrepancy between our notation and the notation used in other results. We thank the KITP for its hospitality, DP acknowledges support from the Charles E. Kaufman Foundation and BK from grant DOE, SciDAC FG02-12ER46875. This research is part of the Blue Waters sustained-petascale computing project, which is supported by the National Science Foundation (award number ACI 1238993) and the state of Illinois. Blue Waters is a joint effort of the University of Illinois at Urbana-Champaign and its National Center for Supercomputing Applications.

Note added: during the preparation of this manuscript we became aware of a complementary work Ref.[35].

[1] P. W. Anderson, Phys. Rev. **109**, 1492 (1958).
[2] E. Abrahams, P. W. Anderson, D. C. Licciardello, and T. V. Ramakrishnan, Phys. Rev. Lett. **42**, 673 (1979).
[3] D. M. Basko, I. L. Aleiner, and B. L. Altshuler, Annals of Physics **321**, 1126 (2006).
[4] D. M. Basko, I. L. Aleiner, and B. L. Altshuler, Phys. Rev. B **76**, 052203 (2007).
[5] V. Oganesyan and D. A. Huse, Phys. Rev. B **75**, 155111 (2007).
[6] M. Žnidarič, T. Prosen, and P. Prelovšek, Phys. Rev. B **77**, 064426 (2008).
[7] C. Monthus and T. Garel, Phys. Rev. B **81**, 134202 (2010).
[8] D. A. Huse, R. Nandkishore, V. Oganesyan, A. Pal, and S. L. Sondhi, Phys. Rev. B **88**, 014206 (2013).
[9] M. Serbyn, Z. Papić, and D. A. Abanin, Phys. Rev. Lett. **111**, 127201 (2013).
[10] D. A. Huse, R. Nandkishore, and V. Oganesyan, Phys. Rev. B **90**, 174202 (2014).
[11] K. Agarwal, S. Gopalakrishnan, M. Knap, M. Mueller, and E. Demler, Phys. Rev. Lett. **114**, 160401 (2015).
[12] A. Pal and D. A. Huse, Phys. Rev. B **82**, 174411 (2010).
[13] B. Bauer and C. Nayak, J. Stat. Mech. **2013**, P09005 (2013).
[14] S. Iyer, V. Oganesyan, G. Refael, and D. A. Huse, Phys. Rev. B **87**, 134202 (2013).
[15] J. A. Kjall, J. H. Bardarson, and F. Pollmann, Phys. Rev. Lett. **113**, 107204 (2014).
[16] J. H. Bardarson, F. Pollmann, and J. E. Moore, Phys. Rev. Lett. **109**, 017202 (2012).
[17] R. Vasseur, S. Parameswaran, and J. Moore, Phys. Rev. B **91**, 140202 (2015).
[18] Y. Bar Lev, G. Cohen, and D. R. Reichman, Phys. Rev. Lett. **114**, 100601 (2015).
[19] B. Swingle, arXiv:1307.0507 (2013).
[20] R. Vosk and E. Altman, Phys. Rev. Lett. **110**, 067204 (2013).
[21] R. Vosk and E. Altman, Phys. Rev. Lett. **112**, 217204 (2014).
[22] M. Friesdorf, A. H. Werner, W. Brown, V. B. Scholz, and J. Eisert, Phys. Rev. Lett. **114**, 170505 (2015).
[23] D. Pekker, G. Refael, E. Altman, E. Demler, and V. Oganesyan, Phys. Rev. X **4**, 011052 (2014).
[24] U. Schollwöck, Annals of Physics **326**, 96 (2011).
[25] T. Devakul and R. R. P. Singh, Phys. Rev. Lett. **115**, 187201 (2015).
[26] R. E. Burkard and U. Derigs, Assignment and Assignment and Matching Problems (Springer-Verlag Berlin, 1980).
[27] In constructing the MPO representation U we used the standard singular value decomposition method with a threshold – singular values below the threshold were dropped. All data presented in the manuscript were collected with the threshold set to 0.01. We tested that decreasing the threshold to 0.001 did not significantly affect the data. Specifically, there was no quantifiable affect on the localization length nor the transition point.
[28] M. S. L. du Croo de Jongh, J. M. J. van Leeuwen, and W. van Saarloos, Phys. Rev. B **62**, 14844 (2000).
[29] A. W. Sandvik and G. Vidal, Phys. Rev. Lett. **99**, 220602 (2007).
[30] L. Wang, I. Pizorn, and F. Verstraete, Phys. Rev. B **83**, 134421 (2011).
[31] C.-P. Chou, F. Pollmann, and T.-K. Lee, Phys. Rev. B **86**, 041105 (2012).
[32] B. K. Clark and H. J. Changlani, arXiv:1404.2296 (2014).
[33] F. Pollmann, V. Khemani, J. I. Cirac, and S. L. Sondhi, Phys. Rev. B **94**, 041116 (2016).
[34] T. B. Wahl, A. Pal, and S. H. Simon, arXiv:1609.01552 (2016).
[35] A. Chandran, I. Carrasquilla, Kim, D. Abanin, and G. Vidal, Phys. Rev. B **92**, 024201 (2015).